主 题:	Your Submission EAAI-24-4012R2	
发件人:	"Engineering Applications of Artificial Intelligence" <em@editorialmanager.com>	2024-12-4 21:59:31
收件人:	"Zhenchang Zhang" <stdin@fafu.edu.cn>	

Dear Prof. Dr. Zhenchang Zhang,

Your manuscript **EAAI-24-4012R2**, entitled "Multi-level domain adaptation for improved generalization in electroencephalogram-based driver fatigue detection" by Prof. Dr. Zhenchang Zhang, Fuzhong Huang; Qicong Wang, Ph.D.; Lei Chen; Wang Mei; Zelong Chen, which you submitted to the International Scientific Journal Engineering Applications of Artificial Intelligence was recommended to me for publication.

I have the pleasure of informing you that I will follow this recommendation and that your paper has been forwarded to the Publishers.

We sincerely appreciate having been given the opportunity to consider this manuscript.

Yours sincerely,

Patrick Siarry
Editor In Chief.
Engineering Applications of Artificial Intelligence

Comments to Authors:

Reviewer #1: This paper demonstrates a clear advancement compared to its previous version. In particular, the enhanced specificity in the comparison analysis is impressive. This improvement significantly strengthens the credibility and reproducibility of the research.

Considering the potential impact of the proposed study on both academia and practical applications, I look forward to its substantial contribution to the advancement of the field.

Reviewer #4: Thanks for the revision. I'm satisfied with the author's response to my comment, even though they provided more details throughout the response file. The overall quality of the manuscript has improved now.

For further assistance, please visit our customer support site at http://help.elsevier.com/app/answers/list/p/7923. Here you can search for solutions on a range of topics, find answers to frequently asked questions and learn more about EM via interactive tutorials. You will also find our 24/7 support contact details should you need any further assistance from one of our customer support representatives

At Elsevier, we want to help all our authors to stay safe when publishing. Please be aware of fraudulent messages requesting money in return for the publication of your paper. If you are publishing open access with Elsevier, bear in mind that we will never request payment before the paper has been accepted. We have prepared some guidelines (https://www.elsevier.com/connect/authors-update/seven-top-tips-on-stopping-apc-scams) that you may find helpful, including a short video on Identifying fake acceptance letters (https://www.youtube.com/watch?v=o5l8thD9XtE). Please remember that you can contact Elsevier s Researcher Support team (https://service.elsevier.com/app/home/supporthub/publishing/) at any time if you have questions about your manuscript, and you can log into Editorial Manager to check the status of your manuscript (https://service.elsevier.com/app/answers/detail/a_id/29155/c/10530/supporthub/publishing/kw/status/).

#AU_EAAI#

To ensure this email reaches the intended recipient, please do not delete the above code

---

Highlights

Multi-level domain adaptation for improved generalization in electroencephalogram-based driver fatigue detection

Fuzhong Huang,Qicong Wang,Lei Chen,Wang Mei,Zhenchang Zhang,Zelong Chen

- Multi-level domain adaptation can extract more general knowledge.

- Improved inter-domain alignment method based on Wasserstein distance.

- Proposed a novel intra-domain contrastive discrepancy to measure intra-domain differences.

- Achieved high generalization performance in cross-subject driving fatigue detection.

- Provides a new direction for driver fatigue detection work.

Multi-level domain adaptation for improved generalization in electroencephalogram-based driver fatigue detection

Fuzhong **Huang**[a], Qicong **Wang**[b], Lei **Chen**[a], Wang **Mei**[a], Zhenchang **Zhang**[a,*] and Zelong **Chen**[c,*]

[a]*College of Computer and Information Sciences, Fujian Agriculture and Forestry University, Fuzhou, 350002, China*
[b]*Department of Computer Science and Technology, Xiamen University, Xiamen, 361005, China*
[c]*Department of Biomedical engineering, 900th hospital of Joint Logistics Support Force, Fuzhou, 350025, China*

ARTICLE INFO

ABSTRACT

Developing a universal model capable of effective cross-subject fatigue detection is crucial for alerting fatigued drivers in a timely manner and reducing traffic accidents. Although existing domain adaptation methods can reduce distribution differences between subjects, they primarily focus on inter-subject feature (inter-domain) alignment while neglecting category-level feature (intra-domain) alignment. To address this issue, this paper proposes a novel Multi-Level Domain Adaptation (MLDA) algorithm to enhance the model's generalization ability on unseen data. Specifically, for inter-domain alignment, we employ an improved Wasserstein distance, whose smooth properties more accurately measure inter-domain differences. For intra-domain alignment, we introduce intra-domain contrastive discrepancy, which enhances the discriminability of category features by maximizing inter-class distances and minimizing intra-class distances. The proposed method achieves cross-subject fatigue detection accuracies of 0.943 and 0.843 on the SEED-VIG and SADT public datasets, respectively. Experimental results demonstrate that MLDA offers significant advantages in cross-subject fatigue detection tasks, providing a promising solution for a generalized driver fatigue detection system.

1. Introduction

Mental fatigue refers to a poor mental state caused by excessive exertion or lack of sufficient rest. Fatigue reduces alertness and concentration, making it one of the leading causes of traffic accidents. Studies have shown that approximately 20%-30% of traffic accidents are related to fatigued driving, and nearly half of all drivers have experienced driving while fatigued (Duhou et al., 2010). Timely alerting drivers before fatigue-induced accidents occur can significantly reduce accident rates (Coetzer and Hancke, 2011). Therefore, researching efficient fatigue detection methods and improving their performance and stability holds great practical significance.

In previous studies, numerous scholars have proposed various models and methods for fatigue detection, which can be mainly categorized into subjective and objective approaches (Sikander and Anwar, 2018). Subjective methods typically assess the fatigue state of subjects through questionnaires, with commonly used scales including the stanford sleepiness scale (Kim and Young, 2005) and the karolinska sleepiness scale (Åkerstedt et al., 1994). Although these methods are easy to administer, they are highly subjective, leading to lower reliability in detection results. Objective methods are divided into two types: computer vision-based and physiological signal-based methods. Computer vision methods evaluate fatigue by assessing indicators such as eye closure duration (Sigari et al., 2013), percentage of eyelid closure (PERCLOS) (Mandal et al.,

---

2017), head posture (Lee et al., 2019), and yawning frequency, or indirectly reflect the driver's fatigue state through abnormal vehicle behaviors, such as lane deviation, steering wheel angle (SWA) (Li et al., 2017), speed, seat load distribution, and changes in brake and throttle pressure (Kamti and Iqbal, 2022). Despite their good performance, these methods are prone to ambiguity. For example, talking with one's mouth open may not indicate fatigue but could be misjudged as a sign of fatigue, affecting the accuracy of detection results.

With the development of brain-computer interface (BCI) technology, direct information exchange between computers and the human brain has become possible, leading to significant applications in various fields such as sleep stage classification (Wang et al., 2023), emotion recognition (Li et al., 2024b), motor imagery (Dang et al., 2024), and epilepsy detection (Tasci et al., 2023). Electroencephalogram (EEG) signals are closely related to fatigue states, providing a stable and reliable reflection of an individual's level of fatigue, and thus have been widely used in driving fatigue detection. To improve detection performance, researchers have proposed various methods. Early studies primarily focused on classifying fatigue states using features such as EEG spectral characteristics (Jap et al., 2009), chaotic entropy (Chaudhuri and Routray, 2020), differential entropy, and power spectral density (Zheng and Lu, 2017). Later, traditional machine learning methods, such as support vector machines (SVM) (Guo et al., 2017), autoregressive (AR) models, and bayesian neural networks (BNN) (Chai et al., 2016), were introduced in this field. To further enhance model performance and simplify feature extraction, deep learning methods have gradually been adopted, including convolutional neural networks (CNN), long short-term memory (LSTM) networks (Stancin et al., 2021), graph convolutional networks (GCN) (Jia et al., 2023; Bai et al., 2021), and generative adversarial networks (GAN) (Jiao et al., 2020). These studies have provided essential support for the continuous advancement of driving fatigue detection technology.

However, an important challenge in the practical application of driver fatigue detection technology is the generalization capability of models. Although the aforementioned methods have achieved good performance, most are based on simulated driving data and assume that all subjects' data are independently and identically distributed. Due to individual differences, these methods may experience a sharp decline in performance in real driving scenarios (Shen et al., 2022). Employing domain adaptation (DA) methods to enhance the model's generalization capability is a promising direction (Zheng and Lu, 2016). DA improves detection performance on unknown data (target domain, unlabeled data) by learning generalized knowledge from existing labeled subject data (source domain). The core idea of DA is to map the source and target domains to the same feature space and minimize the difference in feature distribution between them using some metric. This approach allows the discriminator trained on source domain features to also apply to target domain data, thereby enhancing the model's generalization ability (Kouw and Loog, 2019).

Some researchers have successfully applied single-source DA methods to address the domain shift problem; however, due to data distribution differences between individuals, using data from a single source domain may lead to suboptimal performance (Li et al., 2018b,a). In response, researchers have proposed multi-source DA methods, which have demonstrated excellent discriminative performance in cross-subject fatigue detection (Luo and Lu, 2021). Regarding within-domain adaptation, existing studies typically use Jensen-Shannon (JS) divergence (Menéndez et al., 1997) and Kullback-Leibler (KL) divergence to measure the differences between two domains. However, in high-dimensional spaces, when two distributions do not overlap or the overlapping portion is negligible, JS divergence and KL divergence (Van Erven and Harremos, 2014) can exhibit abrupt changes, which is detrimental to gradient optimization during backpropagation. For within-domain alignment, commonly used methods like maximum mean discrepancy (MMD) (Long et al., 2015; Zhang et al., 2024) or joint maximum mean discrepancy (JMMD) (Long et al., 2017) assess domain differences at the domain level but overlook sample-level differences related to specific classes, thereby somewhat limiting model performance. In summary, the issues present in the aforementioned research can be summarized as follows:

1. Existing research primarily focuses on aligning the distributions of entire domains while neglecting the differences between categories. This results in the model failing to adequately consider the feature differences among various classes during the domain adaptation process, ultimately affecting performance.

2. Current methods for measuring inter-domain differences have limitations in capturing these differences, especially when there are complex nonlinear relationships between domains or when differences exist in high-dimensional spaces. The effectiveness of these methods may be restricted under such conditions.

To tackle the aforementioned issues, this paper proposes a novel multi-level domain adaptation (MLDA) method for cross-subject driver fatigue detection models based on EEG signals. Unlike previous domain adaptation methods, as shown in Fig. 1, our multi-level domain alignment method aligns not only between the source and target domains but also achieves intra-domain alignment at the category level, thereby enhancing model performance. For inter-domain alignment, we employ the Wasserstein distance (Adler and Lunz, 2018) to measure the differences between the source and target domains. The smooth properties of the Wasserstein distance overcome the limitations of JS divergence and KL divergence in reflecting proximity and abrupt changes, effectively measuring the distribution differences between the two domains. Regarding intra-domain alignment, inspired by Kang et al. (2020), we introduce intra-domain contrastive difference to assess the intra-domain alignment discrepancies. This method minimizes intra-class differences while maximizing inter-class differences. Through multi-level domain adaptation, the model captures rich information at different levels, learning more general knowledge and more discriminative features from the source domain, thereby improving the model's generalization ability. In summary, our contributions can be outlined as follows:

1. A multi-level domain adaptation method is introduced for the first time in cross-subject EEG-based fatigue detection. MLDA facilitates domain alignment at both inter-domain and intra-domain levels, allowing the model to acquire more generalizable knowledge and extract more discriminative features.

2. For inter-domain adaptation, to reduce alignment errors caused by abrupt changes and improve the accuracy of inter-domain feature alignment, we propose an improved alignment method based on the Wasserstein distance. The smooth characteristics of the Wasserstein distance optimally measure inter-domain differences.

3. For intra-domain adaptation, addressing the shortcomings of existing domain alignment methods in class alignment, we propose a novel intra-domain contrastive discrepancy approach. This method maximizes inter-class differences while minimizing intra-class distances, making class features easier to distinguish.

4. Extensive experimental results demonstrate that the proposed method achieves excellent performance on various publicly available datasets, providing a new direction for driver fatigue detection.

The remaining sections of this paper are structured as follows. Section 2 provides an overview of relevant work in driver fatigue detection using EEG signals. Section 3 elaborates on the multi-level domain adaptation approach in detail. Experimental results and analysis are presented in Section 4. Section 5 offers a comprehensive discussion of the research conducted in this paper. Finally, Section 6 summarizes the work presented herein.

2. Related works

2.1. Domain adaptation

Domain adaptation is suitable for addressing the problem of distribution mismatch or domain shift between the source domain and target domain, which has numerous applications in machine learning and
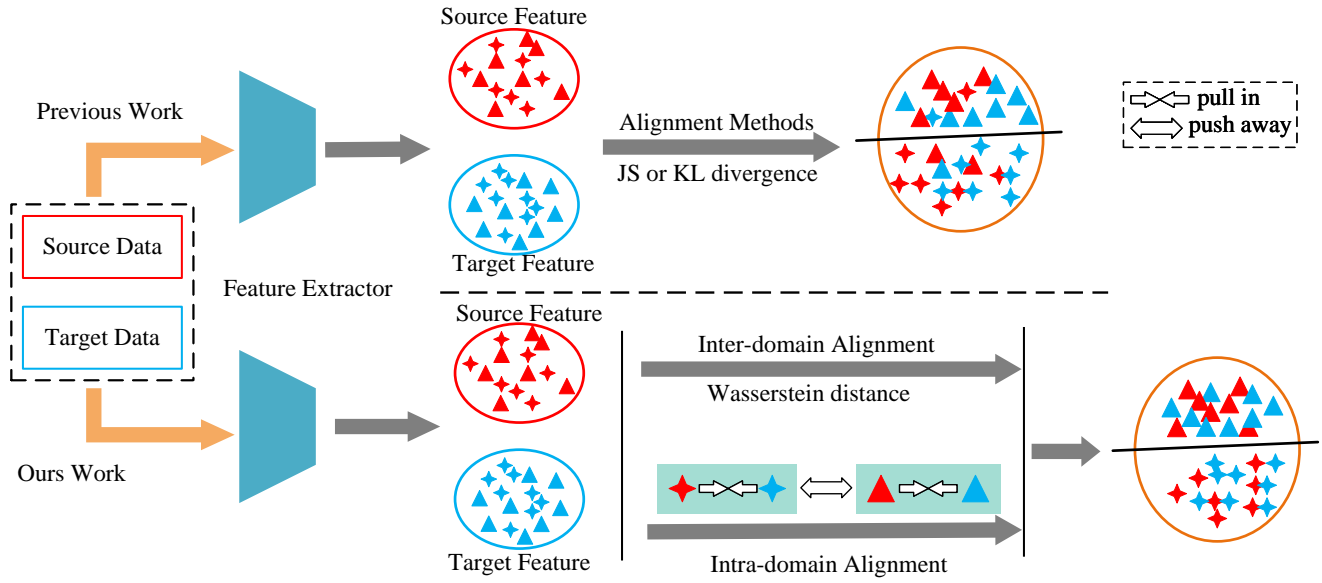
Figure 1: Comparison between previous domain adaptation methods and our method. Previous methods only aligned domains at the inter-domain level, neglecting class-level alignmen. Our work improves inter-domain alignment and, on this basis, minimizes intra-class differences and maximizes inter-class differences to achieve intra-domain alignment.

deep learning tasks (Du et al., 2024; Xu et al., 2024; Gu et al., 2024). DA encompasses semi-supervised domain adaptation (SSDA) and unsupervised domain adaptation (UDA), where SSDA refers to having supervised information in the source domain data (Qiao et al., 2023), and partially supervised information in the target domain data, while UDA refers to having supervised information in the source domain data and no supervised information in the target domain data (Zhang et al., 2023a). Generally, DA methods can be classified into two categories: distance-based methods and adversarial learning-based methods (Qiao et al., 2023).

Distance-based methods explicitly calculate the distribution distance between the source domain and target domain and minimize the distance between them to enhance the model's generalization ability. Long et al. (2015) proposed using a variant of MMD to measure distribution discrepancies, employing the optimal multi-kernel selection method of Mean Embedding Matching to reduce errors. In subsequent research, Long et al. (2017) introduced the JMMD, which measures the Hilbert-Schmidt norm of the empirical joint distribution between the source and target domains. Ge et al. (2023) proposed a conditional maximum mean discrepancy (CMMD) by embedding conditions into the reproducing kernel Hilbert space to measure differences between conditional distributions, thus enabling stable model training and rapid convergence. Using MMD to measure the source and target domains may result in misalignment, but since MMD has been minimized, Kang et al. (2020) proposed contrastive domain discrepancy (CDD) to minimize intra-class differences and maximize inter-class differences at the category level, thereby achieving alignment between the source and target domains while minimizing contrastive domain discrepancy. Zhou et al. (2024) proposed a method for aligning distributions twice through a disentangling and reconstructing process. This method uses a shared feature extraction network for both the source and target domains to obtain the raw extracted features. Then, it disentangles the domain-invariant features and domain-specific features from the raw extracted features. R. et al. (2024) proposed a multi-kernel contrastive domain adaptation for time series classification (MNEMONIC) approach, which integrates statistical feature alignment, contrastive learning, and regularization. This model learns the intrinsic relationships between non-monotonic time data points and aligns the domains into a shared subspace, thereby reducing distribution differences.

Adversarial learning-based methods achieve domain alignment by implicitly training a discriminator. Ganin et al. (2016) designed domain adversarial neural networks (DANN), which employs gradient reversal training to force the network to learn a representation that can predict source domain labels without informing the model of the data's origin from the source or target domain, thereby reducing dependence on the domain and improving performance on the target domain. Building upon this, Li et al. (2018c) proposed bi-directional domain adversarial neural networks (Bi-DANN) for sentiment recognition. The model employs a global domain discriminator and two local domain discriminators, which adversarially work against the classifier, learning unique features of the two brain hemispheres while attempting to reduce domain differences between the source and target domains, thereby enhancing the model's performance. Additionally, Li et al. (2020) introduced a novel bi-hemisphere difference model, which aims to combine differences between the two human brain hemispheres and extract higher-level features, while using a domain discriminator to adversarially induce feature learning modules to learn emotion-related but domain-invariant features to enhance the model's sentiment recognition capability. Lee et al. (2024) proposed a domain adversarial learning network for imbalanced data to address the coexistence of class imbalance and domain shift. This network reduces domain shift by implementing domain adversarial training to learn domain-invariant features and employs a label-aligned sampling strategy to handle class imbalance. Yan et al. (2024) proposed a novel uncertainty-inspired unsupervised domain adaptation (UIUDA) framework, which employs domain adversarial learning to align the feature distributions of training and testing data, enhancing the generalization capability of deep learning models on data with distribution differences.

Despite the considerable research progress achieved by the aforementioned methods, there is still room for improvement in several aspects, such as aligning domains at multiple levels of features or improving the measurement standards for distribution differences between the source and target domains.

2.2. Driver fatigue detection based on EEG

EEG signals, containing inherent signals related to fatigue processes, are effective indicators for fatigue detection (Harvy et al., 2022). Methods for EEG-based fatigue detection can be categorized into those based on individual subjects and those based on cross-subjects.

In studies focusing on individual subjects, Gao et al. (2019) extracted differential entropy (DE) and power spectral density (PSD) from different frequency bands to guide the construction of convolutional neural networks (CNNs), proposing a novel, simple, and effective CNN structure that achieved significant accuracy in fatigue driving detection tasks. Fan et al. (2021) extracted multiple features, including energy, entropy, rhythmic energy ratio, and frontal asymmetry ratio, from prefrontal EEG signals of drivers for fatigue detection. Zhang et al. (2021) applied wavelet thresholding to denoise subjects' EEG data and classified their fatigue states using a combination of CNN and LSTM. Zhang et al. (2023b) proposed a method for multi-dimensional feature selection and fusion based on EEG signals to identify drivers' mental fatigue. Xu et al. (2021) improved fatigue classification performance and computational efficiency by combining CNN with an attention mechanism for analyzing collected simulated driving data.

In cross-subject studies, Zou et al. (2020) detected fatigue using both EEG signals and partial data of steering wheel operations, employing perceptron and logistic regression methods to conduct cross-session and cross-subject experiments on extracted features, showing that data segments during steering wheel manipulation contain valuable information. Cui et al. (2022a) proposed a compact and interpretable convolutional neural network to discover shared EEG features among different subjects for driver fatigue detection. Zeng et al. (2020) introduced an improved transfer learning method based on EasyTL (Wang et al., 2019) for cross-subject fatigue detection using EEG signals. Li et al. (2023) utilized an ensemble deep random vector functional link network for cross-subject driver fatigue detection. Luo and Lu (2021) used Wasserstein distance to measure distribution differences between domains and proposed a multi-source adversarial domain adaptation network for fatigue driving detection. Gao et al. (2023) designed

Table 1
Symbols and the corresponding descriptions.

Symbol	Description
x	Sample
y	Label
$\hat{y}$	Predicted label
θ	Parameters
f	Feature
N	Number of samples
M	Number of classes
DE	Differential entropy feature
$\mathcal{D}_s/\mathcal{D}_t$	Source / target data
$\mathcal{D}_t^l/\mathcal{D}_t^u$	Target labeled/unlabeled data
$P_s(X)/P_t(X)$	Marginal distribution of source/targe
$P_s(Y\vert X)/P_t(Y\vert X)$	Conditional distribution of source/target

a spatiotemporal multi-dimensional feature fusion network using gaussian temporal networks and pure convolutional spatial frequency domain networks for cross-subject fatigue detection. Ma et al. (2019) introduced domain generalization methods to reduce the impact of subject variability, thereby reducing the model's dependence on target domain data.

3. Methodology

The generalization ability of models poses a challenge to their real-world deployment. DA methods address this challenge by projecting both the source domain and target domain data into a common feature subspace. This enables the direct application of knowledge learned from the source domain to the target domain, thus enhancing the model's generalization ability. For ease of description, some symbols used in this paper are listed in Table 1.

In DA research, training samples and testing samples are drawn from two distinct data distributions. Generally, the source domain data $\mathcal{D}_s = \{(x_{si}^l, y_{si}^l)\}_{i=1}^{N_s}$ is sampled from the source domain distribution $P_s(X, Y)$ and comes with labels. Meanwhile, the target domain data $D_t = \{(x_{ti}^u)\}_{i=1}^{N_t}$ is sampled from the target domain distribution $P_t(X, Y)$ and lacks labels. In SSDA problems, some target domain data comes with labels $\mathcal{D}_t^l = \{(x_{ti}^l, y_{ti}^l)\}_{i=1}^{N_t^l}$, denoted as $D_t = \{(x_{ti}^l, y_{ti}^l)\}_{i=1}^{N_t^l} \cup \{(x_{ti}^u)\}_{i=1}^{N_t}$. In this study, the distributions of source domain data and target domain data adhere to the condition of having the same conditional distribution but differing marginal distributions, denoted as $P_s(X) = P_t(X)$ and $P_s(Y\vert X) \neq P_t(Y\vert X)$, respectively.

Fig. 2 illustrates the proposed multi-level domain adaptation framework. As depicted in the figure, MLDA primarily consists of two modules, namely, the feature extractor $\mathcal{G}$ and the classifier $\mathcal{F}$. The network structure of feature extractor $\mathcal{G}$ is illustrated in Fig. 3, and $\mathcal{F}$ denotes fully connected layers. Initially, we extract the differential entropy features from both the source domain data and the target domain data, yielding the differential entropy features DE_s for the source domain and DE_t for the target domain. These features undergo feature extraction via the feature extractor $\mathcal{G}$, resulting in the source domain features f_s and the target domain features f_t. Subsequently, f_s and the target domain data features f_t serve as inputs to the classifier $\mathcal{F}$, generating predictions $\hat{\mathbf{y}}_s^l$ for the source domain data and predictions $\hat{\mathbf{y}}_t^l$ and $\hat{\mathbf{y}}_t^u$ for the target domain data, where the labeled predictions $\hat{\mathbf{y}}_t^l$ for the target domain only appear in SSDA experiments. The computational formulas for this process are defined as

$$\hat{\mathbf{y}}_v^l = \mathcal{F}(\mathbf{f}_v) = \mathcal{F}\Big(\mathcal{G}(DE_v)\Big), v = s, t \tag{1}$$
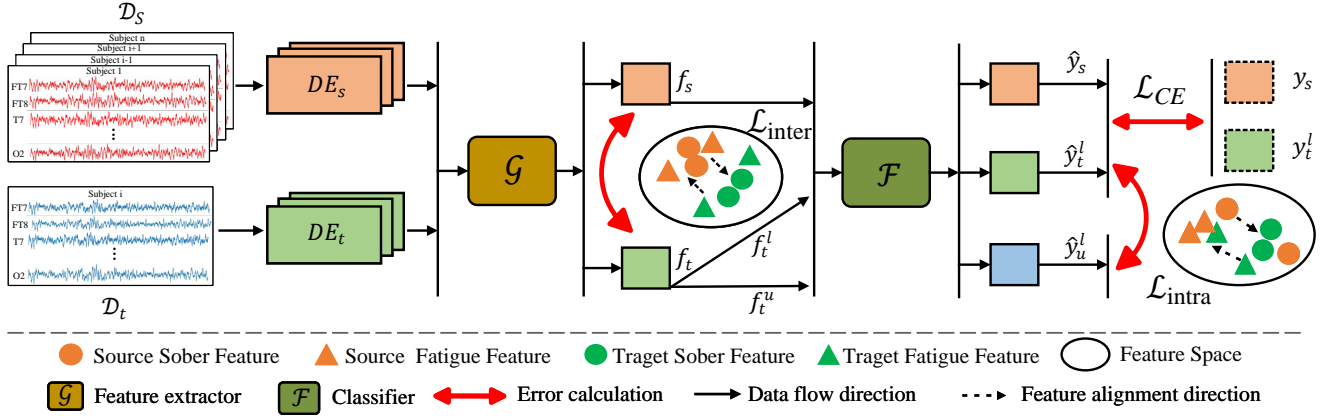
Figure 2: The MLDA framework primarily consists of a feature extractor and a classifier. (i) First, DE features are extracted from both the source and target domains. These features are processed by the feature extractor, while domain differences are computed simultaneously. (ii) The extracted features are then fed into the classifier to generate prediction probabilities, and errors are calculated based on the true values, alongside intra-domain difference calculations. (iii) Finally, backpropagation is applied to optimize the model parameters.
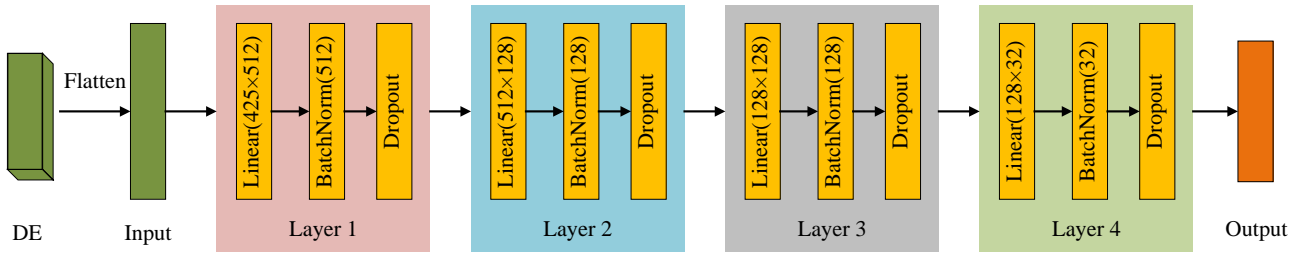

Figure 3: The network architecture of feature extractor $\mathcal{G}$.

To fully utilize the labeled information, we employ the method of minimizing the cross-entropy loss between the predicted values and the true label values to train and optimize the model. The computational formula for this is defined as

$$\min_{\theta_G, \theta_F} \mathcal{L}_{CE} = -\sum_{(x,y)} y \log\left(p(x)\right) \tag{2}$$

Where $\mathcal{L}_{CE}$ represents the labeled cross-entropy loss, θ_G and θ_F denote the parameters of the feature extractor and classifier, respectively, and $p(x)$ is the predicted value for the corresponding data x. Additionally, as described in the subsequent text, our approach performs DA at multiple levels within the feature space to exploit both inter-domain and intra-domain information from the target domain, thereby enhancing the model's generalization capability.

3.1. Preprocessing

Temporal information can intuitively illustrate the changes of signals over time, facilitating understanding. However, certain signals may exhibit highly complex behaviors in the time domain, making it challenging to extract useful information from them. Duan et al. (2013) proposed differential entropy(DE) as an effective EEG feature for fatigue state recognition and emotion recognition. Compared to traditional measures such as power density and time-domain features, this feature demonstrates superior performance. Therefore, in this study, we adopt the DE features of EEG signals as inputs to the model.

In general, if a variable X is approximately Gaussian distributed with distribution $N(\mu, \sigma^2)$, then the DE features of variable X can be calculated using the following formula:

$$DE(X) = - \int_{-\infty}^{\infty} \varphi(x) \log(\varphi(x)) \, dx = \frac{1}{2} \log 2\pi e \sigma^2 \tag{3}$$

where

$$\varphi(x) = \frac{1}{\sqrt{2\pi\sigma^2}} \exp \frac{(x-\mu)^2}{2\sigma^2} \tag{4}$$

We denote μ as the mean of variable X, and σ as the standard deviation of variable X. Employing data from EEG signals ranging from 1 to 50Hz, we extract the DE features of EEG signals at a frequency of 2Hz.

3.2. Inter-domain alignment

In high-dimensional spaces, when the source domain and target domain data do not overlap or the overlapping parts can be ignored, traditional metrics such as KL divergence and JS divergence fail to accurately reflect the distance between the two domains. This situation leads to discontinuities, rendering the gradient optimization mechanism of deep learning infeasible. To address this issue, at the domain level, we introduce the optimal transport distance, also known as the Wasserstein distance, to measure the discrepancy between domains. The Wasserstein distance exhibits smoothness, enabling meaningful gradients and thereby providing a more accurate reflection of the differences between domains.

The alignment between two domains is modeled as an optimal transport problem (Courty et al., 2016). The goal of inter-domain alignment is to determine an optimal transport plan γ^* that minimizes the transportation cost between the feature distributions of the source and target domains. Formally, the cost of this process can be defined as

$$E(P_s, P_t) = \inf \langle \mathbf{D}, \mathbf{\Gamma} \rangle_F \tag{5}$$

Where P_s and P_t represent the marginal distributions of the source domain and target domain respectively, Π denotes all joint distributions between the source and target domains, $\langle \cdot, \cdot \rangle_F$ denotes the Frobenius inner product. $D = \|u - v\|$ represents the distance between features of the source and target domains, $\mathbf{\Gamma} = \gamma(u, v)$ represents the transportation plan sampled from the joint distribution Π, i.e., $\gamma \sim \Pi(P_s, P_t)$, γ is related to the sampled results. E represents the transportation cost, used to measure the difference between the feature distributions of the source and target domains. Thus, we can define the difference between the source and target domains.

$$\begin{aligned} \mathcal{L}_{inter} &= \inf_{\gamma \in \Pi} \sum_{u,v} \|\xi_s(u) - \xi_t(v)\| \gamma(u, v) \\ &= \inf \mathbb{E}_{(u,v)\sim\gamma} \|\xi_s(u) - \xi_t(v)\| \end{aligned} \tag{6}$$

Where $\xi(\cdot)$ denotes a fully c onnected neural network. By employing backpropagation and gradient updates, the inter-domain difference $\mathcal{L}_{inter}$ can be reduced, leading to the optimal transportation plan γ^* that minimizes the difference between the source and target domains.

3.3. Intra-domain alignment

Assuming two sets of observed data X and Y are independently and identically distributed according to p and q respectively, the MMD can readily discern whether p and q are of the same distribution. The

principle behind MMD is that if two distributions are identical, sampling from them and applying any arbitrary mapping should result in equal expectations after mapping. Formally, MMD is defined as

$$D(p, q) = \sup_{f \in B} \left(\mathbf{E}_p \left[f(x) \right] - \mathbf{E}_q \left[f(y) \right] \right) \tag{7}$$

where f is a mapping function, and B is the unit ball in the universal reproducing kernel hilbert space (RKHS) (Gretton et al., 2012). In practical computations, the square of MMD is commonly used as an empirical estimate.

$$
\begin{aligned}
D^2(p, q) &= \left\| \frac{1}{m} \sum_{i=1}^{m} k(x_i, \cdot) - \frac{1}{n} \sum_{j=1}^{n} k(y_j, \cdot) \right\|^2 \\
&= \frac{1}{m^2} \sum_{i,j=1}^{m} k(x_i, x_j) - \frac{2}{mn} \sum_{i,j=1}^{m,n} k(x_i, y_j) + \frac{1}{n^2} \sum_{i,j=1}^{n} k(y_i, y_j)
\end{aligned}
\tag{8}
$$

Building upon the aforementioned foundation and inspired by Kang et al. (2020), at the intra-domain level, an intra-domain contrastive discrepancy is proposed, aiming to minimize intra-class distance while maximizing inter-class distance. For any two identical or different categories, c_1 and c_2, formally, the distance between them can be defined as

$$D_{c_1 c_2}(\{\hat{y}_{ti}\}_{i=1}^{N_t}, \phi) = D_1 + D_2 - 2D_3 \tag{9}$$

where

$$D_1 = \sum_{i=1}^{N_s} \sum_{j=1}^{N_s} \frac{\mu_{c_1 c_1}(y_{si}, y_{sj}) k(\phi_\theta(x_{si}), \phi_\theta(x_{sj}))}{\sum_{i=1}^{N_s} \sum_{j=1}^{N_s} \mu_{c_1 c_1}(y_{si}, y_{sj})} \tag{10}$$

$$D_2 = \sum_{i=1}^{N_t} \sum_{j=1}^{N_t} \frac{\mu_{c_2 c_2}(\hat{y}_{ti}, \hat{y}_{tj}) k(\phi_\theta(x_{ti}), \phi_\theta(x_{tj}))}{\sum_{i=1}^{N_t} \sum_{j=1}^{N_t} \mu_{c_2 c_2}(\hat{y}_{ti}, \hat{y}_{tj})} \tag{11}$$

$$D_3 = \sum_{i=1}^{N_s} \sum_{j=1}^{N_t} \frac{\mu_{c_1 c_2}(y_{si}, \hat{y}_{tj}) k(\phi_\theta(x_{si}), \phi_\theta(x_{tj}))}{\sum_{i=1}^{N_s} \sum_{j=1}^{N_t} \mu_{c_1 c_2}(y_{si}, \hat{y}_{tj})} \tag{12}$$

$$\mu_{cc'}(y, y') = \begin{cases} 1 & \text{if } y = c, y' = c' \\ 0 & \text{otherwise.} \end{cases} \tag{13}$$

where $k(\cdot, \cdot)$ denotes the kernel function, which is used to construct kernel embeddings of the source and target domains to compute the distance between these two points. $\phi(\cdot)$ represents the function mapping. when $c_1 = c_2 = c$, D_{cc} represents intra-class disparity, and when $c_1 \neq c_2$, $D_{c_1 c_2}$ represents inter-class disparity. Therefore, we can obtain the intra-domain contrastive discrepancy, and the computational formula is defined as

$$\mathcal{L}_{intra} = \frac{1}{M} D_{intra} - \frac{1}{M(M-1)} D_{inter} \tag{14}$$

where

$$D_{intra} = \sum_{c=1}^{M} D_{cc}(\{\hat{y}_{ti}\}_{i=1}^{N_t}, \phi) \tag{15}$$

$$D_{inter} = \sum_{c=1}^{M} \sum_{c'=1, c' \neq c}^{M} \mathcal{D}_{cc'}(\{\hat{y}_{ti}\}_{i=1}^{N_t}, \phi) \tag{16}$$

D_{intra} represents intra-class variance, while D_{intra} represents inter-class variance. Adding opposite coefficients to D_{intra} and D_{inter} enables them to optimize towards opposite directions.

3.4. Overall objective function

As a result, the overall objective function can be defined as

$$\min_{\theta} \mathcal{L} = \mathcal{L}_{CE} + \lambda \mathcal{L}_{inter} + (1 - \lambda) \mathcal{L}_{intra} \tag{17}$$

where

$$\lambda = \frac{e^{(-N+100)}}{1 + e^{(-N+100)}} \tag{18}$$

Introducing a parameter between $\mathcal{L}_{inter}$ and $\mathcal{L}_{intra}$ can adjust the balance between them.

4. Experiments

4.1. Dataset

The effectiveness of the proposed method is validated on two datasets: the SEED-VIG dataset and the Sustained-Attention Driving Task (SADT) dataset.

4.1.1. Introduction of SEED-VIG dataset

SEED-VIG (Zheng and Lu, 2017) is a publicly available EEG dataset widely used for driving fatigue detection, provided by the Brain-Computer-Machine Intelligence Research Center at Shanghai Jiao Tong University (SJTU). The data collection experiment involves 21 participants with an average age of 23.3, who engage in simulated driving within virtual reality scenarios that encompass various weather and road conditions. The total duration of the experiment is 118 minutes, during which EEG signals are recorded using the Neuroscan system at a sampling frequency of 1000 Hz, later resampled to 200 Hz, with a total of 17 channels. The raw EEG signal dimensions for each participant are 17 (channels) × 1,416,000 (sampling points). The experiment measures participants' fatigue alertness using the PERCLOS index, which represents the percentage of time the eyes are closed within a given period (ranging from 0 to 1). The calculation formula for PERCLOS is as follows:

$$PERCLOS = \frac{blink + close}{interval} \tag{19}$$

Where, $blink$, $close$, and $interval$ represent the blink duration, eye closure duration, and total duration of the experiment, respectively.

4.1.2. Introduction of SADT dataset

SADT (Cao et al., 2019) is a continuous attention task conducted in a 90-minute immersive driving simulator, provided by the Brain Research Center at National Chiao Tung University (NCTU). The experimental data is collected from 27 participants aged between 22 and 28. During the experiment, participants are required to keep the car centered in a four-lane highway while random lane deviation events (deviation onset) occur, prompting them to react immediately (response onset) and compensate for the disturbance by steering the car back to the center lane (response offset). A complete trial consists of the three events: deviation onset, response onset, and response offset. EEG signals are collected using a wired EEG cap with 32 Ag/AgCl electrodes, comprising 30 EEG electrodes and 2 reference electrodes, recording each participant's brain activity according to the international 10-20 system, with a sampling rate of 500 Hz, and preprocessed using a bandpass filter of 1-50 Hz and artifact suppression.

4.2. Experimental design

To evaluate the performance of the proposed method in cross-subject fatigue detection, leave-one-subject cross-validation (LOSO) experiments are conducted, along with two sets of experiments: semi-supervised multi-level domain adaptation (SMLDA) and unsupervised multi-level domain adaptation (UMLDA). This section provides a detailed description of the data processing, evaluation metrics, and implementation details.

4.2.1. Data preprocessing

For the SEED-VIG dataset, we classify the data into awake and fatigue categories based on the PERCLOS value, using a threshold of 0.35, and select data from 12 participants with relatively balanced sample sizes. Each participant's experimental duration is 8 seconds, resulting in 885 samples. Differential entropy feature extraction is performed on the EEG signals using Eq. (3), with each participant's EEG signal DE features consisting of 25 frequency bands. Ultimately, the data shape for each participant's EEG signals is 885 (samples) $\times$ 17 (channels) $\times$ 25 (frequency bands).

For the SADT dataset, we use the preprocessed data. Following the method of Yuan et al. (2024), we label the data using local reaction time and global reaction time. Local reaction time is the interval from deviation onset to reaction onset, while global reaction time is calculated by averaging the reaction times of all trials within 90 seconds before an impending deviation event. Any participant data with fewer than 50 samples in any category is discarded, resulting in data from 11 participants, totaling 2,022 EEG signal samples. Each EEG signal sample has a shape of 30 (channels) $\times$ 384 (sampling points), and the shape of the frequency domain feature-extracted data is 30 (channels) $\times$ 25 (frequency bands).

In SMLDA experiment, 80% of a randomly selected subject sample is used as the test set, while the remaining 20% of samples and all other subject samples are used as the training and validation sets. The specific steps of the experiment are detailed in Algorithm 1. In UMLDA experiment, one subject sample is selected as the test set to validate the model's generalization performance, while the remaining subject samples are used for model training and validation. The specific steps are outlined in Algorithm 2.

4.2.2. Comparison methods and metrics

To enable effective comparison, we compare the proposed method with 10 existing EEG-based cross-subject fatigue detection models from three perspectives: non-domain adaptation (non-DA), semi-supervised domain adaptation (SSDA), and unsupervised domain adaptation (UDA). Non-DA methods include EEGNet (Lawhern et al., 2018), ICNN (Cui et al., 2022b), Conformer (Song et al., 2023), ICNN+FGloWD (Li et al., 2023), and TFormer (Li et al., 2024a), with ICNN+FGloWD being the SOTA method for non-DA on the SEED-VIG dataset, and TFormer being the SOTA method for non-DA on the SADT dataset. SSDA methods utilize partial label information from the target domain, such as subject matching (SM) (Li et al., 2022). UDA methods include SHOT (Liang et al., 2020), DINE (Liang et al., 2021), BBUDA (Liu et al., 2022), and SPARK (Yuan et al., 2024), with SPARK being the SOTA method for cross-fatigue detection in UDA.

Algorithm 1 Semi-supervised multi-level domain adaptation.

Require: Source data $\mathcal{D}_s$, $\mathcal{D}_t^l$, target data $\mathcal{D}_t^u$, epoch N, learning
   rate lr, batch size bs and hyperparameters λ;
Output:
   Predicted values of the target data;
Ensure:
 1: **for** $(n \leftarrow 1; n \leq N; n \leftarrow n+1)$ **do**
 2:     Sampling source samples $\{(x_{si}^l, y_{si}^l)\}_{i=1}^{bs}$ from $\mathcal{D}_s$ and $\mathcal{D}_t^l$;
 3:     Sampling target samples $\{(x_{ti}^u, y_{ti}^u)\}_{i=1}^{bs}$ from $\mathcal{D}_t^u$;
 4:     Using $\mathcal{G}$ to compute f_s, f_t^l and f_t^u;
 5:     Computing $\mathcal{L}_{inter}$ using Eq. (6);
 6:     Computing $\mathcal{L}_{intra}$ using Eq. (14);
 7:     Using $\mathcal{F}$ to compute $\hat{\mathbf{y}}_s^l$, $\hat{\mathbf{y}}_t^l$ and $\hat{\mathbf{y}}_t^u$;
 8:     Using $\mathbf{y}_s^l$, $\mathbf{y}_t^l$, $\hat{\mathbf{y}}_s^l$, $\hat{\mathbf{y}}_t^l$ to compute $\mathcal{L}_{CE}$;
 9:     Backpropagating errors with the objective $\mathcal{L}$;
10:     Updating the parameters θ of MLDA.
11: **end for**

Algorithm 2 Unsupervised multi-level domain adaptation.

Require: Source data $\mathcal{D}_s$, target data $\mathcal{D}_t$, epoch N, learning rate
   lr, batch size bs and hyperparameters λ;
Output:
   Predicted values of the target data;
Ensure:
 1: **for** $(n \leftarrow 1; n \leq N; n \leftarrow n+1)$ **do**
 2:     Sampling source samples $\{(x_{si}^l, y_{si}^l)\}_{i=1}^{bs}$ from $\mathcal{D}_s$;
 3:     Sampling target samples $\{(x_{ti}^u, y_{ti}^u)\}_{i=1}^{bs}$ from $\mathcal{D}_t$;
 4:     Using $\mathcal{G}$ to compute f_s and f_t;
 5:     Computing $\mathcal{L}_{inter}$ using Eq. (6);
 6:     Computing $\mathcal{L}_{intra}$ using Eq. (14);
 7:     Using $\mathcal{F}$ to compute $\hat{\mathbf{y}}_s^l$ and $\hat{\mathbf{y}}_t^u$;
 8:     Using $\mathbf{y}_s^l$, $\hat{\mathbf{y}}_s^l$ to compute $\mathcal{L}_{CE}$;
 9:     Backpropagating errors with the objective $\mathcal{L}$;
10:     Updating the parameters θ of MLDA.
11: **end for**

Accuracy and F1-score are used as metrics to evaluate the model's performance, with the calculation formulas as follows:

$$Accuracy = \frac{TP + TN}{TP + FP + FN + TN} \tag{20}$$

$$F1\text{-}score = \frac{2 \times Precision \times Recall}{Precision + Recall} \tag{21}$$

$$Precision = \frac{TP}{TP + FP} \tag{22}$$

$$Recall = \frac{TP}{TP + FN} \tag{23}$$

where, TP, TN, FP, and FN represent true positives (correctly identified fatigue states), true negatives (correctly identified awake states), false positives (incorrectly identified fatigue states), and false negatives (incorrectly identified awake states), respectively.

4.2.3. Implementation details

In the experiments, we ensure the uniqueness of sample selection and the reproducibility of results by setting a random seed. The SGD optimizer is used during training, with a learning rate set to 5×10^{-3}. In the SEED-VIG dataset experiments, the batch size is 128, while in the SADT dataset experiments, the batch size is 64, with a total of 600 training epochs. The model implementation is based on Python 3.8.18 and PyTorch 1.12.1, and training and testing are conducted on a GeForce RTX 2080 Ti GPU. Code is available at *https://github.com/Rebond/MLDA*

However, the complexity of the model may lead to the risk of overfitting. To mitigate this risk, we implement several measures. First, we incorporate Dropout layers in each layer of the feature extractor, randomly dropping a portion of the neurons with a dropout rate set between 5% and 45%. Additionally, we set the $weight\_decay$ parameter in the SGD optimizer to 5×10^{-4}, applying decay during each model parameter update to prevent overfitting. During the training phase, we employ early stopping, monitoring accuracy on the test set to select the best training model.

4.3. Experimental results and comparison

Table 2 and Table 3 present the experimental results of the proposed MLDA method and the comparison methods for cross-subject fatigue detection on two datasets. It is observed that MLDA demonstrates the best performance among all the comparison methods. Additionally, SMLDA outperforms UMLDA on both datasets. Specifically, on the SEED-VIG dataset, the accuracy of MLDA is at least 0.8% higher than other methods, while SMLDA exceeds UMLDA by 6%. On the SADT dataset, the accuracy of MLDA is at least 3.2% higher than other methods, and SMLDA outperforms UMLDA by 0.9%. The reason for MLDA achieving the best performance lies in its use of a multi-level domain adaptation mechanism, which not only performs overall inter-domain alignment but also conducts more refined alignment at the category level, significantly enhancing category discriminability. This multi-level alignment strategy enables the model to better capture feature differences across different categories, thereby improving the accuracy of cross-subject detection. The advantage of SMLDA over UMLDA is that it incorporates partially labeled information from the target domain for training, allowing the model to better adapt to the characteristics of the target domain. By utilizing this labeled information, SMLDA more effectively captures the common features across subjects, reducing the bias caused by insufficient samples. As a result, SMLDA demonstrates stronger effectiveness and reliability in practical applications. Next, the research findings will be further discussed from three aspects.

4.3.1. Comparison with non-DA methods

Comparing the experimental results in Table 2 and Table 3, it is encouraging to find that the proposed MLDA method outperforms the non-DA methods on both datasets. Specifically, on the SEED-VIG dataset, the accuracy of MLDA for cross-subject fatigue detection is 2.4% higher than the SOTA method ICNN+FGloWD and improves by 3% to 14.2% compared to other methods. On the SADT dataset, MLDA's

Table 2
Comparison results of LOSO fatigue detection on SEED-VIG dataset. "Avg. Acc." denotes average accuracy, and "Std." represents standard deviation. **Bold** indicates the best result, and underline indicates the second-best result.

Method	Subject												Avg. Acc.	Std.
	1	2	3	4	5	6	7	8	9	10	11	12		
EEGNet(Lawhern et al., 2018)	0.855	0.611	0.710	0.711	0.799	0.780	0.805	0.852	0.787	0.938	0.860	0.893	0.800	0.0901
ICNN(Cui et al., 2022b)	0.952	0.895	0.892	0.846	0.851	0.950	0.849	0.923	0.933	0.920	0.871	0.903	0.899	0.0382
Conformer(Song et al., 2023)	0.861	0.858	0.750	0.794	0.929	0.859	0.795	0.824	0.791	0.847	0.673	0.823	0.817	0.0644
ICNN+FGloWD(Li et al., 2023)	0.947	0.938	0.887	0.885	0.959	0.946	0.838	0.979	0.936	0.920	0.881	0.898	0.918	0.0403
TFormer(Li et al., 2024a)	0.959	0.937	0.885	0.869	0.965	0.960	0.840	0.954	0.916	0.922	0.851	0.885	0.912	0.0446
SHOT(Liang et al., 2020)	0.978	0.934	0.894	0.880	0.984	0.992	0.837	0.965	0.950	0.963	0.883	0.901	0.930	0.0498
DINE(Liang et al., 2021)	0.996	0.934	0.872	0.908	0.990	0.974	0.821	0.965	0.980	0.966	0.862	0.892	0.930	0.0578
SM(Li et al., 2022)	0.930	0.920	0.874	0.854	0.928	0.954	0.717	0.972	0.911	0.923	0.910	0.898	0.899	0.0655
BBUDA(Liu et al., 2022)	0.969	0.946	0.851	0.878	0.985	0.989	0.816	0.978	0.933	0.953	0.878	0.880	0.923	0.0583
SPARK(Yuan et al., 2024)	0.982	0.952	0.876	0.900	0.990	0.998	0.829	0.965	0.943	0.965	0.910	0.904	0.934	0.0512
UMLDA(Ours)	0.881	0.854	0.869	0.938	0.818	0.953	0.849	0.896	0.920	0.870	0.907	0.823	0.882	0.0428
SMLDA(Ours)	0.945	0.903	0.932	0.965	0.946	0.961	0.915	0.968	0.915	0.958	0.969	0.932	**0.942**	**0.0227**

Table 3
Comparison results of LOSO fatigue detection on SADT dataset. **Bold** indicates the best result, and underline indicates the second-best result.

Method	Subject											Avg. Acc.	Std.
	1	2	3	4	5	6	7	8	9	10	11		
EEGNet(Lawhern et al., 2018)	0.564	0.720	0.467	0.655	0.536	0.639	0.677	0.538	0.717	0.796	0.584	0.627	0.0982
ICNN(Cui et al., 2022b)	0.851	0.456	0.800	0.777	0.915	0.855	0.657	0.811	0.889	0.657	0.699	0.761	0.1344
Conformer(Song et al., 2023)	0.754	0.611	0.736	0.688	0.858	0.836	0.602	0.697	0.776	0.739	0.734	0.731	0.0801
ICNN+FGloWD(Li et al., 2023)	0.872	0.606	0.827	0.791	0.906	0.855	0.677	0.792	0.905	0.750	0.734	0.794	0.0946
TFormer(Li et al., 2024a)	0.802	0.799	0.764	0.803	0.893	0.859	0.655	0.761	0.844	0.789	0.797	0.797	**0.0616**
SHOT(Liang et al., 2020)	0.898	0.773	0.800	0.777	0.875	0.928	0.657	0.807	0.893	0.806	0.704	0.811	0.0837
DINE(Liang et al., 2021)	0.888	0.788	0.813	0.757	0.872	0.914	0.686	0.795	0.892	0.778	0.708	0.808	0.0760
SM(Li et al., 2022)	0.787	0.682	0.793	0.682	0.853	0.837	0.647	0.572	0.780	0.824	0.717	0.743	0.0894
BBUDA(Liu et al., 2022)	0.894	0.773	0.813	0.770	0.888	0.897	0.657	0.799	0.886	0.713	0.695	0.799	0.0861
SPARK(Yuan et al., 2024)	0.910	0.833	0.813	0.777	0.897	0.910	0.659	0.822	0.889	0.685	0.712	0.810	0.0914
UMLDA(Ours)	0.851	0.909	0.813	0.777	0.897	0.813	0.735	0.799	0.936	0.917	0.721	0.834	0.0742
SMLDA(Ours)	0.894	0.868	0.817	0.849	0.894	0.842	0.707	0.769	0.933	0.943	0.757	**0.843**	0.0748

accuracy is 4.6% higher than the SOTA method TFormer, with improvements of 4.9% to 21.6% over other methods. This result can be attributed to the fact that different subjects may exhibit distribution differences in their data during cross-subject fatigue detection. MLDA addresses this by adjusting the feature space to uncover common features between the source and target domains. In contrast, methods that do not use domain adaptation, such as ICNN+FGloWD and TFormer, while possessing strong feature extraction capabilities, lack mechanisms to handle domain differences, making them less effective in addressing issues related to inconsistent data distributions and resulting in reduced accuracy in cross-subject detection.

4.3.2. Comparison with SSDA model

As shown in Table 2 and Table 3, compared to semi-supervised methods such as the SM method, the proposed MLDA method achieves an average accuracy that is 4.3% and 10% higher on the SEED-VIG and SADT datasets, respectively. This advantage can be attributed to two main factors. First, MLDA uses DE features as input, which are effective for detecting fatigue states, while the SM method utilizes raw EEG signals as input, leading to insufficient extraction of frequency domain features. Second, the SM method

collects statistical information from the source domain during the training phase and computes the distance between the source and target domains for subject matching during the testing phase, resulting in inadequate utilization of information from the target domain. In contrast, MLDA leverages partially labeled target domain data for model training, effectively uncovering invariant features between the target and source domains, thereby enhancing the model's performance.

4.3.3. Comparison with UDA methods

The experimental results in Table 2 and Table 3 indicate that UDA methods, such as SPARK, achieve good performance in cross-subject fatigue detection. However, the proposed MLDA method still surpasses SPARK in accuracy by 0.8% and 3% on the SEED-VIG and SADT datasets, respectively, and improves at least 1.2% and 3.2% compared to other unsupervised domain adaptation methods. This significant enhancement arises from the fact that methods like SPARK only perform a coarse alignment of the overall feature space of subjects, neglecting detailed alignment at the category level. In contrast, MLDA builds on inter-domain alignment by further considering intra-domain alignment. This category-level feature alignment enables the model to learn more generalizable knowledge from the target domain, enhancing its generalization capability. Moreover, during the category-level alignment process, MLDA maximizes inter-class differences while minimizing intra-class differences through the introduction of intra-domain contrastive discrepancy, further improving the discernibility of fatigue features. These factors collectively contribute to the significant performance improvement of MLDA in cross-subject fatigue detection.

4.4. Ablation study

We conducted ablation experiments to evaluate the effectiveness of intra-domain and inter-domain adaptation in the proposed method. The experiments include two settings: setting $\lambda = 1$ in the Eq. (17) means that backpropagation is unaffected by inter-domain adaptation. Setting $\lambda = 0$ means that backpropagation is unaffected by intra-domain adaptation.

Effect of inter-domain alignmen: Table 4 presents the results of the ablation experiments for MLDA on the two datasets. The results indicate a decline in both accuracy and F1-score when inter-domain adaptation is not employed. SMLDA w/o. Inter shows a decrease of 0.7% in accuracy and F1-score on the SEED-VIG dataset, and a decrease of 0.9% and 1% on the SADT dataset, respectively. UMLDA w/o. Inter shows declines of 2.2% and 2.4% in accuracy and F1-score on the SEED-VIG dataset, and decreases of 4% and 0.5% on the SADT dataset, respectively. This performance decline can be attributed to the critical role of inter-domain alignment in reducing the distribution differences between the source and target domains. By effectively aligning the features of the source and target domains, MLDA captures common features and enhances the model's adaptability. Without inter-domain alignment, the model struggles to learn the features of the target domain and faces difficulties due to feature bias, resulting in decreased classification performance. Therefore, inter-domain alignment is essential for improving the model's performance and generalization ability.

Effect of intra-domain alignment: From Table 4, it is observed that SMLDA w/o. Intra performs worse than SMLDA on both datasets, with the smallest decreases in accuracy and F1-score on the SEED-VIG dataset being 0.7% and 0.3%, respectively. Surprisingly, UMLDA w/o. Intra shows a more significant performance decline, with accuracy dropping by 4% and 4.1% on the SADT dataset. This difference can be attributed to the fact that MLDA effectively reduces intra-class differences through category-level feature alignment, enhancing the model's discernibility of category features. While the model can still maintain a certain level of performance without intra-domain alignment, the lack of detailed alignment of category-level features significantly reduces its adaptability to target domain features, resulting in greater accuracy loss on the SADT dataset. This highlights the critical importance of intra-domain alignment for improving the model's discernibility and generalization ability; the absence of this mechanism directly impacts the model's performance.

Table 4
Ablation study results of MLDA on SEED-VIG and SADT datasets. "w/o. Inter" indicates that inter-domain adaptation effects are not considered, while "w/o. intra" indicates that intra-domain adaptation effects are not considered.

Dataset	Method	Accuracy ± Std.	F1-score ± Std.
SEED-VIG	SMLDA	**0.942 ± 0.0227**	**0.938 ± 0.0254**
	SMLDA w/o. Inter	0.935 ± 0.0227	0.931 ± 0.0282
	SMLDA w/o. Intra	0.934 ± 0.0216	0.935 ± 0.0212
	UMLDA	0.882 ± 0.0428	0.872 ± 0.0510
	UMLDA w/o. Inter	0.860 ± 0.0523	0.848 ± 0.0601
	UMLDA w/o. Intra	0.814 ± 0.0724	0.817 ± 0.0647
SADT	SMLDA	**0.843 ± 0.0748**	**0.842 ± 0.0763**
	SMLDA w/o. Inter	0.834 ± 0.0868	0.832 ± 0.0888
	SMLDA w/o. Intra	0.807 ± 0.0754	0.803 ± 0.0799
	UMLDA	0.834 ± 0.0742	0.832 ± 0.0762
	UMLDA w/o. Inter	0.829 ± 0.0865	0.827 ± 0.0886
	UMLDA w/o. Intra	0.794 ± 0.0759	0.791 ± 0.0786

Table 5
Comparison experiment results of different numbers of subjects in the source domain on the SEED-VIG dataset. "$A \rightarrow B$" indicates that the source and target domain have A and B participants respectively.

Method	Accuracy ± Std.	F1-score ± Std.
SMLDA(11→1)	0.942 ± 0.0227	0.938 ± 0.0254
SMLDA(21→1)	0.897 ± 0.0574	0.893 ± 0.0599
UMLDA(11→1)	0.882 ± 0.0428	0.872 ± 0.0510
UMLDA(21→1)	0.848 ± 0.0768	0.830 ± 0.0884

In summary, the analysis results indicate that both inter-domain and intra-domain alignment have a positive impact on model performance, with intra-domain alignment contributing more significantly to performance improvement compared to inter-domain alignment. Removing either alignment mechanism leads to a decline in model performance, while effectively combining both mechanisms allows the model to achieve optimal performance.

4.5. Sensitivity analysis
To investigate the influence of other factors on model performance, a sensitivity analysis was conducted, specifically exploring three aspects: the number of subjects in the source domain, different metric approaches, and varying input features.

4.5.1. Analysis of the number of subjects in the source domain
In the SEED-VIG dataset, we conducted experiments with 11 and 21 subjects in the source domain. Table 5 presents the experimental results for different numbers of source domain subjects. The results indicate that SMLDA(11→1) has an accuracy that is 4.55% higher than SMLDA(21→1), while UMLDA(11→1) has an accuracy that is 3.31% higher than UMLDA(21→1). This suggests that increasing the number of subjects in the source domain does not always have a positive impact on model performance. Specifically, when the number of subjects in the source domain is small, the model is more effective at capturing common features among subjects. Additionally, a smaller sample size reduces data diversity, making it easier for the

Table 6
Comparison results of inter-domain alignment using different measurement methods on the SEED-VIG dataset. WD represents Wasserstein distance, JS represents Jensen-Shannon divergence, and KL represents Kullback-Leibler divergence. "w" indicates "with".

Method	Accuracy $\pm$ Std.	F1-score $\pm$ Std.
MLDA w. WD	0.942 $\pm$ 0.0227	0.938 $\pm$ 0.0254
MLDA w. KL	0.897 $\pm$ 0.0574	0.893 $\pm$ 0.0599
MLDA w. JS	0.882 $\pm$ 0.0428	0.872 $\pm$ 0.0510

Table 7
Comparison results using different features on the SEED-VIG dataset. DE represents differential entropy and PSD denotes power spectral density.

Method	Accuracy $\pm$ Std.	F1-score $\pm$ Std.
MLDA w. DE	0.882 $\pm$ 0.0428	0.872 $\pm$ 0.0510
MLDA w. PSD	0.824 $\pm$ 0.0471	0.825 $\pm$ 0.0486

model to find effective decision boundaries. In contrast, when the number of subjects in the source domain increases, data diversity rises, which may lead to more complex feature distributions and introduce additional noise. Therefore, moderating the number of subjects in the source domain can help improve the model's performance in the target domain.

4.5.2. Analysis of metric approaches

In addition to using Wasserstein distance, we also selected JS divergence and KL divergence as measures for inter-domain features. The experimental results in Table 6 indicate that MLDA w. WD achieves better cross-subject fatigue detection performance on the SEED-VIG dataset compared to MLDA w. KL and MLDA w. JS, with accuracy higher by 4.5% and 6%, and F1-score higher by 4.5% and 6.6%, respectively. This outcome is attributed to the fact that Wasserstein distance more effectively measures the differences between probability distributions. It not only considers the overall shape of the distributions but also takes into account the specific locations and relative distances of data points in the space, allowing for a more accurate capture of the distribution differences between the source and target domains. In contrast, KL divergence and JS divergence fail to adequately reflect this complex relationship, making it challenging to effectively align feature distributions in certain cases.

4.5.3. Analysis of input features

Both power spectral density (PSD) and differential entropy (DE) can reflect the frequency domain characteristics of EEG signals. To investigate the impact of different frequency domain features on model performance, we conducted unsupervised cross-subject fatigue detection using PSD and DE as input features on the SEED-VIG dataset. The experimental results in Table 7 show that MLDA w. DE outperforms MLDA w. PSD by 5.8% and 4.7% in accuracy and F1-score, respectively. This improvement is attributed to DE's ability to more effectively capture the complexity and uncertainty of signals, particularly when dealing with non-stationary signals. By analyzing the changes in probability distributions, DE better reflects the dynamic characteristics of EEG signals, providing richer information. In contrast, while PSD describes the energy distribution of signals, it is relatively inadequate in capturing time-varying characteristics and complex patterns. Therefore, using DE as an input feature in fatigue detection tasks helps enhance the model's classification performance and generalization capability.

Table 8

Comparison of average processing time.

Method	Accuracy	Time
BBUDA	0.799	6.58s
DINE	0.808	3.97s
SPARK	0.810	1.06s
MLDA	0.843	0.196s

4.6. Analysis of computational efficiency

In this section, we analyze the computational efficiency of the proposed method, MLDA, in detail. MLDA is trained and tested on an Intel Xeon Silver 4110 2.1GHz CPU and a GeForce RTX 2080 Ti GPU, with a software environment of Python 3.8.18, PyTorch 1.12.1, and CUDA 11.4. Table 8 presents a comparison of processing times between MLDA and other unsupervised domain adaptation (UDA) methods, showing that our method significantly reduces the average processing time. This improvement mainly results from MLDA calculating inter-domain and intra-domain differences only during the training phase to facilitate network learning, while no such calculations are required during the testing phase, thereby accelerating the inference process.

4.7. Visualization

To provide a clearer understanding of the alignment process of MLDA, we record the feature changes during the experiments and visualize them using t-SNE (Van der Maaten and Hinton, 2008). Fig. 4 displays the visualization results, where three different experimental feature datasets are selected, with each row representing the results of one experiment. In each row, the distribution changes of fatigue and alertness state features in the source and target domains are shown from left to right, corresponding to different stages of domain adaptation. From the figure, it is observed that before domain adaptation, there is significant overlap in the feature distributions of the source and target domains, with no clear boundaries between features, making it impossible to distinguish between fatigue and alertness states using a simple linear separation plane. During the domain adaptation process, MLDA's inter-domain alignment strategy progressively aligns the features of the source and target domains, while intra-domain contrast minimizes intra-class features and maximizes inter-class features. Ultimately, after the domain adaptation is complete, the features of fatigue and alertness states are well-separated, allowing effective classification using a simple linear classifier. This process intuitively demonstrates the advantages of MLDA in cross-domain fatigue detection tasks, as the inter-domain and intra-domain alignment mechanisms enhance the distinguishability of features.

5. Discussion

We propose a multi-level domain adaptation algorithm, MLDA, which achieves superior cross-subject fatigue detection performance on the SEED-VIG and SADT public datasets. Based on the detailed comparisons and visual analyses from the previous section, we conclude that MLDA can further align at the category level on top of inter-domain feature alignment, enabling the model to learn more target domain knowledge and achieve better performance in cross-subject fatigue detection. Additionally, we set up two experimental groups: unsupervised and semi-supervised. When some target domain labels are accessible, SMLDA can be chosen, while UMLDA is suitable when no label information is available. Thus, our method can be flexibly applied in various scenarios.

We conduct a comparative analysis of the proposed MLDA method against existing deep learning approaches from three perspectives: non-DA methods, SSDA methods, and UDA methods. First, compared
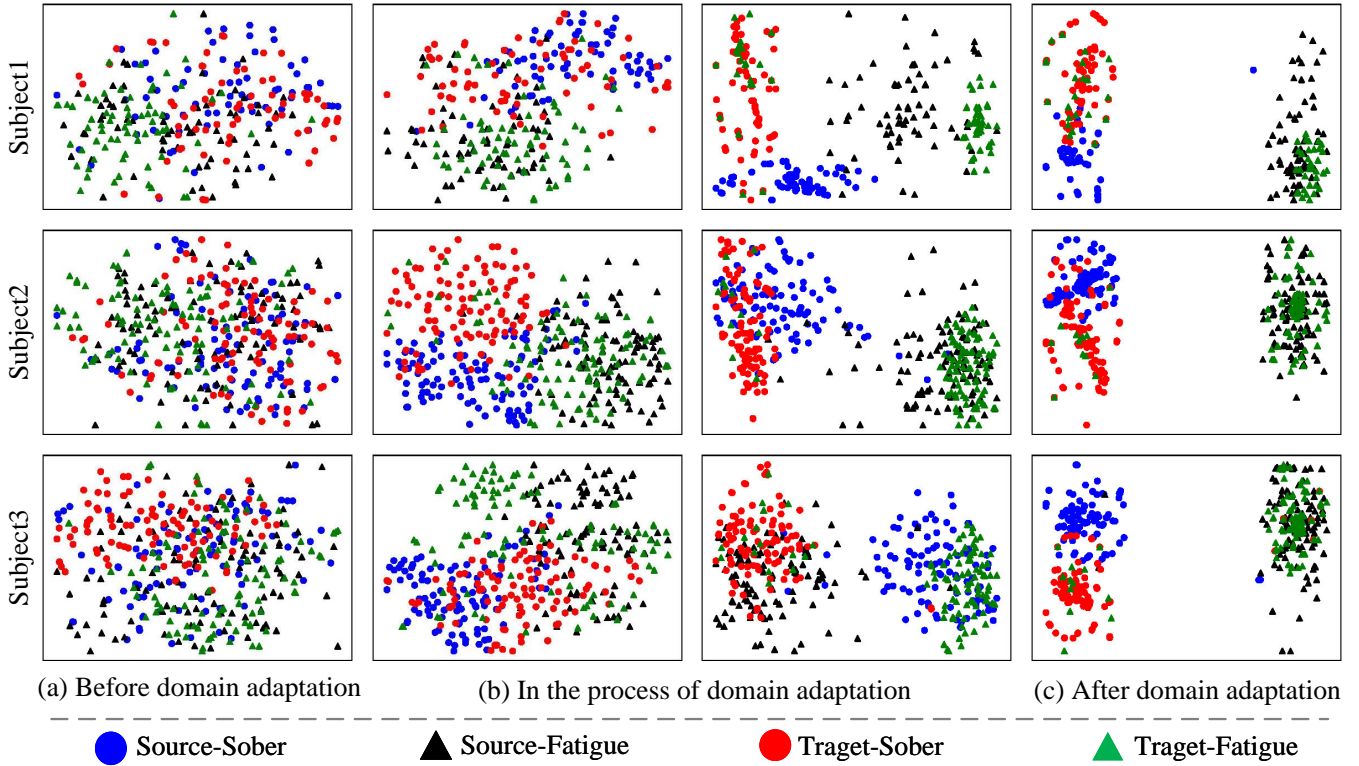
Multi-level domain adaptation for improved generalization in EEG-based driver fatigue detection

(a) Before domain adaptation   (b) In the process of domain adaptation   (c) After domain adaptation

● Source-Sober   ▲ Source-Fatigue   ● Traget-Sober   ▲ Traget-Fatigue

Figure 4: Using t-SNE to visualize the features of the source domain and target domain. (a) Before domain adaptation, there is significant overlap between the features of the source domain and the target domain. (b) During domain adaptation, the source and target domains gradually become aligned. (c) After domain adaptation, a simple linear plane can be used to distinguish between fatigue and awake features.

to non-DA methods, which typically train solely on source domain data and lack adaptability to the distribution differences in the target domain, MLDA's advantage lies in its domain alignment strategy, allowing the model to better learn knowledge from the target domain. Second, in comparison with SSDA methods, MLDA makes more effective use of partially labeled target domain data. Finally, when compared to existing UDA methods, such as SPARK, which primarily focus on aligning the overall feature spaces of the source and target domains while neglecting the fine-grained alignment of intra-domain features, MLDA excels not only in inter-domain alignment but also enhances model performance through category-level alignment. The multi-level alignment strategy enables MLDA to capture more information from the target domain, effectively improving the model's classification performance.

Despite the outstanding performance of the proposed MLDA method in cross-subject fatigue detection, the collection and processing of EEG signals in real driving scenarios still face numerous challenges. On one hand, the comfort and portability of EEG devices impose higher requirements for long-term wear by drivers, while factors such as noise, electromagnetic interference, and poor electrode contact during data collection can lead to decreased signal quality. On the other hand, EEG signal processing requires high real-time capabilities to ensure timely and accurate detection of driver fatigue states. Potential solutions to address these challenges include developing lightweight, comfortable, and efficient wearable EEG devices, employing advanced noise suppression and signal enhancement technologies to improve data quality, and incorporating edge computing technologies to reduce latency and enhance real-time processing capabilities. These improvements will effectively promote the practical application of EEG signals in driving fatigue monitoring, enhancing the system's reliability and usability.

6. Conclusion

This paper proposes a multi-level domain adaptation method (MLDA) for cross-subject EEG signal fatigue detection, incorporating both inter-domain and intra-domain adaptation strategies. In terms of inter-domain adaptation, we improve existing alignment methods by employing Wasserstein distance to achieve global alignment of subject features from the source and target domains, thereby reducing inter-domain differences. Intra-domain adaptation is achieved through fine-grained alignment at the category level, where we design an intra-domain contrastive discrepancy mechanism to maximize inter-class distances while minimizing intra-class distances, enhancing categorical discrimination capabilities. Extensive and rigorous experimental results demonstrate that MLDA exhibits outstanding performance across various EEG signal datasets. In future work, we will further explore the fusion of EEG signals with other physiological signals (such as EOG and heart rate variability), subject facial features, and vehicle behavior data, aiming to construct a more universal driving fatigue detection model.

Declaration of interests

The authors declare that they have no known competing financial interests or personal relationships that could have appeared to influence the work reported in this paper.

References

Adler, J., Lunz, S., 2018. Banach wasserstein gan. Advances in neural information processing systems 31. URL: https://dl.acm.org/doi/abs/10.5555/3327757.3327781.

Åkerstedt, T., Hume, K.I., Minors, D.S., Waterhouse, J.M., 1994. The subjective meaning of good sleep, an intraindividual approach using the karolinska sleep diary. Perceptual and Motor Skills 79, 287 – 296. doi:10.2466/pms.1994.79.1.287.

Azab, A.M., Mihaylova, L., Ang, K.K., Arvaneh, M., 2019. Weighted transfer learning for improving motor imagery-based brain–computer interface. IEEE Transactions on Neural Systems and Rehabilitation Engineering 27, 1352–1359. doi:10.1109/TNSRE.2019.2923315.

Bai, J., Yu, W., Xiao, Z., Havyarimana, V., Regan, A.C., Jiang, H., Jiao, L., 2021. Two-stream spatial–temporal graph convolutional networks for driver drowsiness detection. IEEE Transactions on Cybernetics 52, 13821–13833. doi:10.1109/TCYB.2021.3110813.

Cao, Z., Chuang, C.H., King, J.K., Lin, C.T., 2019. Multi-channel eeg recordings during a sustained-attention driving task. Scientific Data 6. doi:10.1038/s41597-019-0027-4.

Chai, R., Naik, G.R., Nguyen, T.N., Ling, S.H., Tran, Y., Craig, A., Nguyen, H.T., 2016. Driver fatigue classification with independent component by entropy rate bound minimization analysis in an eeg-based system. IEEE journal of biomedical and health informatics 21, 715–724. doi:10.1109/JBHI.2016.2532354.

Chaudhuri, A., Routray, A., 2020. Driver fatigue detection through chaotic entropy analysis of cortical sources obtained from scalp eeg signals. IEEE Transactions on Intelligent Transportation Systems 21, 185–198. doi:10.1109/TITS.2018.2890332.

Coetzer, R.C., Hancke, G.P., 2011. Eye detection for a real-time vehicle driver fatigue monitoring system. 2011 IEEE Intelligent Vehicles Symposium (IV) , 66–71doi:10.1109/IVS.2011.5940406.

Courty, N., Flamary, R., Tuia, D., Rakotomamonjy, A., 2016. Optimal transport for domain adaptation. IEEE transactions on pattern analysis and machine intelligence 39, 1853–1865. doi:10.1109/TPAMI.2016.2615921.

Cui, J., Lan, Z., Liu, Y., Li, R., Li, F., Sourina, O., Müller-Wittig, W., 2022a. A compact and interpretable convolutional neural network for cross-subject driver drowsiness detection from single-channel eeg. Methods 202, 173–184. doi:10.1016/j.ymeth.2021.04.017.

Cui, J., Lan, Z., Sourina, O., Müller-Wittig, W., 2022b. Eeg-based cross-subject driver drowsiness recognition with an interpretable convolutional neural network. IEEE Transactions on Neural Networks and Learning Systems doi:10.1109/TNNLS.2022.3147208.

Dang, W., Lv, D., Tang, M., Sun, X., Liu, Y., Grebogi, C., Gao, Z., 2024. Flashlight-net: A modular convolutional neural network for motor imagery eeg classification. IEEE Transactions on Systems, Man, and Cybernetics: Systems 54, 4507–4516. doi:10.1109/TSMC.2024.3382828.

Dasgupta, A., George, A., Happy, S.L., Routray, A., 2013. A vision-based system for monitoring the loss of attention in automotive drivers. IEEE Transactions on Intelligent Transportation Systems 14, 1825–1838. doi:10.1109/TITS.2013.2271052.

Du, Z., Li, X., Li, F., Lu, K., Zhu, L., Li, J., 2024. Domain-agnostic mutual prompting for unsupervised domain adaptation, in: Proceedings of the IEEE/CVF Conference on Computer Vision and Pattern Recognition, pp. 23375–23384. doi:10.48550/arXiv.2403.02899.

Duan, R.N., Zhu, J.Y., Lu, B.L., 2013. Differential entropy feature for eeg-based emotion classification, in: 2013 6th international IEEE/EMBS conference on neural engineering (NER), IEEE. pp. 81–84. doi:10.1109/NER.2013.6695876.

Duhou, L., Qun, L., Wei, Y., Hao-xue, L., 2010. Relationship between fatigue driving and traffic accident. Journal of Traffic and Transportation Engineering 10, 104–109. URL: https://api.semanticscholar.org/CorpusID:112466099.

Fan, C., Peng, Y., Peng, S., Zhang, H., Wu, Y., Kwong, S., 2021. Detection of train driver fatigue and distraction based on forehead eeg: a time-series ensemble learning method. IEEE transactions on intelligent transportation systems 23, 13559–13569. doi:10.1109/tits.2021.3125737.

Ganin, Y., Ustinova, E., Ajakan, H., Germain, P., Larochelle, H., Laviolette, F., March, M., Lempitsky, V., 2016. Domain-adversarial training of neural networks. Journal of machine learning research 17, 1–35. doi:10.1007/978-3-319-58347-1_10.

Multi-level domain adaptation for improved generalization in EEG-based driver fatigue detection

Gao, D., Li, P., Wang, M., Liang, Y., Liu, S., Zhou, J., Wang, L., Zhang, Y., 2023. Csf-gtnet: A novel multi-dimensional feature fusion network based on convnext-gelu-bilstm for eeg-signals-enabled fatigue driving detection. IEEE Journal of Biomedical and Health Informatics doi:10.1109/JBHI.2023.3240891.

Gao, Z., Li, Y., Yang, Y., Dong, N., Yang, X., Grebogi, C., 2019. A coincidence-filtering-based approach for cnns in eeg-based recognition. IEEE Transactions on Industrial Informatics 16, 7159–7167. doi:10.1109/TII.2019.2955447.

Ge, P., Ren, C.X., Xu, X.L., Yan, H., 2023. Unsupervised domain adaptation via deep conditional adaptation network. Pattern Recognition 134, 109088. doi:10.1016/j.patcog.2022.109088.

Gretton, A., Borgwardt, K., Rasch, M., Schölkopf, B., Smola, A., 2006. A kernel method for the two-sample-problem. Advances in neural information processing systems 19. doi:10.7551/mitpress/7503.003.0069.

Gretton, A., Borgwardt, K.M., Rasch, M.J., Schölkopf, B., Smola, A., 2012. A kernel two-sample test. The Journal of Machine Learning Research 13, 723–773. doi:10.5555/2503308.2188410.

Gu, X., Sun, J., Xu, Z., 2024. Unsupervised and semi-supervised robust spherical space domain adaptation. IEEE Transactions on Pattern Analysis and Machine Intelligence 46, 1757–1774. doi:10.1109/TPAMI.2022.3158637.

Guo, Z., Pan, Y., Zhao, G., Cao, S., Zhang, J., 2017. Detection of driver vigilance level using eeg signals and driving contexts. IEEE Transactions on Reliability 67, 370–380. doi:10.1109/TR.2017.2778754.

Harvy, J., Bezerianos, A., Li, J., 2022. Reliability of eeg measures in driving fatigue. IEEE Transactions on Neural Systems and Rehabilitation Engineering 30, 2743–2753. doi:10.1109/TNSRE.2022.3208374.

Jap, B.T., Lal, S., Fischer, P., Bekiaris, E., 2009. Using eeg spectral components to assess algorithms for detecting fatigue. Expert Systems with Applications 36, 2352–2359. doi:10.1016/j.eswa.2007.12.043.

Jia, H., Xiao, Z., Ji, P., 2023. End-to-end fatigue driving eeg signal detection model based on improved temporal-graph convolution network. Computers in Biology and Medicine 152, 106431. doi:10.1016/j.compbiomed.2022.106431.

Jiao, Y., Deng, Y., Luo, Y., Lu, B.L., 2020. Driver sleepiness detection from eeg and eog signals using gan and lstm networks. Neurocomputing 408, 100–111. doi:10.1016/j.neucom.2019.05.108.

Kamti, M.K., Iqbal, R., 2022. Evolution of driver fatigue detection techniques—a review from 2007 to 2021. Transportation Research Record 2676, 485 – 507. doi:10.1177/03611981221096118.

Kang, G., Jiang, L., Wei, Y., Yang, Y., Hauptmann, A., 2020. Contrastive adaptation network for single-and multi-source domain adaptation. IEEE transactions on pattern analysis and machine intelligence 44, 1793–1804. doi:10.1109/TPAMI.2020.3029948.

Kim, H., Young, T.B., 2005. Subjective daytime sleepiness: dimensions and correlates in the general population. Sleep 28 5, 625–34. doi:10.1093/sleep/28.5.625.

Kouw, W.M., Loog, M., 2019. A review of domain adaptation without target labels. IEEE transactions on pattern analysis and machine intelligence 43, 766–785. doi:10.1109/TPAMI.2019.2945942.

Lawhern, V.J., Solon, A.J., Waytowich, N.R., Gordon, S.M., Hung, C.P., Lance, B.J., 2018. Eegnet: a compact convolutional neural network for eeg-based brain–computer interfaces. Journal of neural engineering 15, 056013. doi:10.1088/1741-2552/aace8c.

Lee, J., Ko, J.U., Kim, T., Kim, Y.C., Jung, J.H., Youn, B.D., 2024. Domain adaptation with label-aligned sampling (dalas) for cross-domain fault diagnosis of rotating machinery under class imbalance. Expert Systems with Applications 243, 122910. doi:10.1016/j.eswa.2023.122910.

Lee, K.H., Kim, W., Choi, H.K., Jang, B.T., 2019. A study on feature extraction methods used to estimate a driver's level of drowsiness. 2019 21st International Conference on Advanced Communication Technology (ICACT) , 710–713doi:10.23919/ICACT.2019.8701928.

Li, H., Jin, Y.M., Zheng, W.L., Lu, B.L., 2018a. Cross-subject emotion recognition using deep adaptation networks, in: Neural Information Processing: 25th International Conference, ICONIP 2018, Siem Reap, Cambodia, December 13–16, 2018, Proceedings, Part V 25, Springer. pp. 403–413. doi:10.1007/978-3-030-04221-9_36.

Li, H., Zheng, W.L., Lu, B.L., 2018b. Multimodal vigilance estimation with adversarial domain adaptation networks, in: 2018 International Joint Conference on Neural Networks (IJCNN), IEEE. pp. 1–6. doi:10.1109/IJCNN.2018.8489212.

Li, R., Gao, R., Yuan, L., Suganthan, P., Wang, L., Sourina, O., 2023. An enhanced ensemble deep random vector functional link network for driver fatigue recognition. Engineering Applications of Artificial Intelligence 123, 106237. doi:10.1016/j.engappai.2023.106237.

Li, R., Hu, M., Gao, R., Wang, L., Suganthan, P., Sourina, O., 2024a. Tformer: A time–frequency transformer with batch normalization for driver fatigue recognition. Advanced Engineering Informatics 62, 102575. doi:10.1016/j.aei.2024.102575.

Li, R., Wang, L., Sourina, O., 2022. Subject matching for cross-subject eeg-based recognition of driver states related to situation awareness. Methods 202, 136–143. doi:10.1016/j.ymeth.2021.04.009.

Li, X., Chen, C.L.P., Chen, B., Zhang, T., 2024b. Gusa: Graph-based unsupervised subdomain adaptation for cross-subject eeg emotion recognition. IEEE Transactions on Affective Computing 15, 1451–1462. doi:10.1109/TAFFC.2024.3349770.

Li, Y., Wang, L., Zheng, W., Zong, Y., Qi, L., Cui, Z., Zhang, T., Song, T., 2020. A novel bi-hemispheric discrepancy model for eeg emotion recognition. IEEE Transactions on Cognitive and Developmental Systems 13, 354–367. doi:10.1109/TCDS.2020.2999337.

Li, Y., Zheng, W., Zong, Y., Cui, Z., Zhang, T., Zhou, X., 2018c. A bi-hemisphere domain adversarial neural network model for eeg emotion recognition. IEEE Transactions on Affective Computing 12, 494–504. doi:10.1109/TAFFC.2018.2885474.

Li, Z., Zhang, Q., Zhao, X., 2017. Performance analysis of k-nearest neighbor, support vector machine, and artificial neural network classifiers for driver drowsiness detection with different road geometries. International Journal of Distributed Sensor Networks 13. doi:10.1177/1550147717733391.

Liang, J., Hu, D., Feng, J., 2020. Do we really need to access the source data? source hypothesis transfer for unsupervised domain adaptation, in: International Conference on Machine Learning (ICML), pp. 6028–6039. URL: https://proceedings.mlr.press/v119/liang20a/liang20a.pdf.

Liang, J., Hu, D., Feng, J., He, R., 2021. Dine: Domain adaptation from single and multiple black-box predictors. 2022 IEEE/CVF Conference on Computer Vision and Pattern Recognition (CVPR) , 7993–8003doi:10.1109/CVPR52688.2022.00784.

Liu, X., Yoo, C., Xing, F., Kuo, C.C.J., Fakhri, G.E., Kang, J.W., Woo, J., 2022. Unsupervised domain adaptation for segmentation with black-box source model, in: Medical Imaging. doi:10.1117/12.2607895.

Long, M., Cao, Y., Wang, J., Jordan, M., 2015. Learning transferable features with deep adaptation networks, in: International conference on machine learning, PMLR. pp. 97–105. URL: https://dl.acm.org/doi/10.5555/3045118.3045130.

Long, M., Zhu, H., Wang, J., Jordan, M.I., 2017. Deep transfer learning with joint adaptation networks, in: International conference on machine learning, PMLR. pp. 2208–2217. URL: https://dl.acm.org/doi/10.5555/3305890.3305909.

Luo, Y., Lu, B.L., 2021. Wasserstein-distance-based multi-source adversarial domain adaptation for emotion recognition and vigilance estimation, in: 2021 IEEE International Conference on Bioinformatics and Biomedicine (BIBM), IEEE. pp. 1424–1428. doi:10.1109/BIBM52615.2021.9669383.

Ma, B.Q., Li, H., Zheng, W.L., Lu, B.L., 2019. Reducing the subject variability of eeg signals with adversarial domain generalization, in: Neural Information Processing: 26th International Conference, ICONIP 2019, Sydney, NSW, Australia, December 12–15, 2019, Proceedings, Part I 26, Springer. pp. 30–42. doi:10.1007/978-3-030-36708-4_3.

Van der Maaten, L., Hinton, G., 2008. Visualizing data using t-sne. Journal of machine learning research 9. URL: http://jmlr.org/papers/v9/vandermaaten08a.html.

Mandal, B., Li, L., Wang, G.S., Lin, J., 2017. Towards detection of bus driver fatigue based on robust visual analysis of eye state. IEEE Transactions on Intelligent Transportation Systems 18, 545–557. doi:10.1109/TITS.2016.2582900.

Menéndez, M., Pardo, J., Pardo, L., Pardo, M., 1997. The jensen-shannon divergence. Journal of the Franklin Institute 334, 307–318. doi:10.1016/S0016-0032(96)00063-4.

Pan, S.J., Tsang, I.W., Kwok, J.T., Yang, Q., 2010. Domain adaptation via transfer component analysis. IEEE transactions on neural networks 22, 199–210. doi:10.1109/TNN.2010.2091281.

Qiao, Z., Luo, X., Xiao, M., Dong, H., Zhou, Y., Xiong, H., 2023. Semi-supervised domain adaptation in graph transfer learning. arXiv preprint arXiv:2309.10773 doi:10.24963/ijcai.2023/253.

R., L., Jose, B.R., Mathew, J., Sanodiya, R.K., 2024. Mnemonic: Multikernel contrastive domain adaptation for time-series classification. Engineering Applications of Artificial Intelligence 133, 108255. doi:10.1016/j.engappai.2024.108255.

Shen, X., Liu, X., Hu, X., Zhang, D., Song, S., 2022. Contrastive learning of subject-invariant eeg representations for cross-subject emotion recognition. IEEE Transactions on Affective Computing 14, 2496–2511. doi:10.1109/TAFFC.2022.3164516.

Sigari, M.H., Fathy, M., Soryani, M., 2013. A driver face monitoring system for fatigue and distraction detection. International Journal of Vehicular Technology 2013, 1–11. doi:10.1155/2013/263983.

Sikander, G., Anwar, S., 2018. Driver fatigue detection systems: A review. IEEE Transactions on Intelligent Transportation Systems 20, 2339–2352. doi:10.1109/TITS.2018.2868499.

Song, Y., Zheng, Q., Liu, B., Gao, X., 2023. Eeg conformer: Convolutional transformer for eeg decoding and visualization. IEEE Transactions on Neural Systems and Rehabilitation Engineering 31, 710–719. doi:10.1109/TNSRE.2022.3230250.

Stancin, I., Cifrek, M., Jovic, A., 2021. A review of eeg signal features and their application in driver drowsiness detection systems. Sensors 21, 3786. doi:10.3390/s21113786.

Tasci, I., Taşcı, B., Barua, P.D., Dogan, S., Tuncer, T., Palmer, E., Fujita, H., Acharya, U.R., 2023. Epilepsy detection in 121 patient populations using hypercube pattern from eeg signals. Inf. Fusion 96, 252–268. doi:10.1016/j.inffus.2023.03.022.

Van Erven, T., Harremos, P., 2014. Rényi divergence and kullback-leibler divergence. IEEE Transactions on Information Theory 60, 3797–3820. doi:10.1109/TIT.2014.2320500.

Wang, J., Chen, Y., Yu, H., Huang, M., Yang, Q., 2019. Easy transfer learning by exploiting intra-domain structures, in: 2019 IEEE international conference on multimedia and expo (ICME), IEEE. pp. 1210–1215. doi:10.1109/ICME.2019.00211.

Wang, J., Zhao, S., Zhou, Y., Jiang, H., Yu, Z., Li, T., Li, S., Pan, G., 2023. Narcolepsy diagnosis with sleep stage features using psg recordings. IEEE Transactions on Neural Systems and Rehabilitation Engineering 31, 3619–3629. doi:10.1109/TNSRE.2023.3312396.

Xu, M., Wang, H., Ni, B., 2024. Graphical modeling for multi-source domain adaptation. IEEE Transactions on Pattern Analysis and Machine Intelligence 46, 1727–1741. doi:10.1109/TPAMI.2022.3172372.

Xu, T., Wang, H., Lu, G., Wan, F., Deng, M., Qi, P., Bezerianos, A., Guan, C., Sun, Y., 2021. E-key: An eeg-based biometric authentication and driving fatigue detection system. IEEE Transactions on Affective Computing 14, 864–877. doi:10.1109/TAFFC.2021.3133443.

Yan, Y., Ma, S., Song, K., Wang, Y., Tian, H., Guo, J., 2024. Uncertainty inspired domain adaptation network for rail surface defect segmentation. Engineering Applications of Artificial Intelligence 135, 108860. doi:10.1016/j.engappai.2024.108860.

Yuan, L., Li, R., Cui, J., Siyal, M.Y., 2024. Spark: A high-efficiency black-box domain adaptation framework for source privacy-preserving drowsiness detection. IEEE Journal of Biomedical and Health Informatics 28, 3478–3488. doi:10.1109/JBHI.2024.3377373.

Zeng, H., Zhang, J., Zakaria, W., Babiloni, F., Gianluca, B., Li, X., Kong, W., 2020. Instanceeasytl: An improved transfer-learning method for eeg-based cross-subject fatigue detection. Sensors 20, 7251. doi:10.3390/s20247251.

Zhang, D., Westfechtel, T., Harada, T., 2023a. Unsupervised domain adaptation via minimized joint error. Transactions on Machine Learning Research .

Zhang, S., Zhang, Z., Chen, Z., Lin, S., Xie, Z., 2021. A novel method of mental fatigue detection based on cnn and lstm. International Journal of Computational Science and Engineering 24, 290–300. doi:10.1504/IJCSE.2021.115656.

Zhang, Y., Ding, J., Li, Y., Ren, Z., Feng, K., 2024. Multi-modal data cross-domain fusion network for gearbox fault diagnosis under variable operating conditions. Engineering Applications of Artificial Intelligence 133, 108236. doi:10.1016/j.engappai.2024.108236.

Zhang, Y., Guo, H., Zhou, Y., Xu, C., Liao, Y., 2023b. Recognising drivers' mental fatigue based on eeg multi-dimensional feature selection and fusion. Biomedical Signal Processing and Control 79, 104237. doi:10.1016/j.bspc.2022.104237.

Zheng, W.L., Lu, B.L., 2016. Personalizing eeg-based affective models with transfer learning, in: Proceedings of the twenty-fifth international joint conference on artificial intelligence, pp. 2732–2738. URL: https://dl.acm.org/doi/10.5555/3060832.3061003.

Zheng, W.L., Lu, B.L., 2017. A multimodal approach to estimating vigilance using eeg and forehead eog. Journal of neural engineering 14, 026017. doi:10.1088/1741-2552/aa5a98.

Zhou, L., Ye, M., Li, X., Zhu, C., Liu, Y., Li, X., 2024. Disentanglement then reconstruction: Unsupervised domain adaptation by twice distribution alignments. Expert Systems with Applications 237, 121498. doi:10.1016/j.eswa.2023.121498.

Zou, B., Shen, M., Li, X., Zheng, Y., Zhang, L., 2020. Eeg-based driving fatigue detection during operating the steering wheel data section, in: 2020 42nd Annual International Conference of the IEEE Engineering in Medicine & Biology Society (EMBC), IEEE. pp. 248–251. doi:10.1109/EMBC44109.2020.9175962.